Developmental Biology 416 (2016) 389–401

Contents lists available at ScienceDirect

Developmental Biology

journal homepage: www.elsevier.com/locate/developmentalbiology

The two-step development of a duplex retina involves distinct events of cone and rod neurogenesis and differentiation

Ragnhild Valen [a,*,1], Mariann Eilertsen [a], Rolf Brudvik Edvardsen [b], Tomasz Furmanek [b], Ivar Rønnestad [a], Terje van der Meeren [c], Ørjan Karlsen [c], Tom Ole Nilsen [d], Jon Vidar Helvik [a]

[a] Department of Biology, University of Bergen, NO-5020 Bergen, Norway
[b] Institute of Marine Research, Nordnes, NO-5005 Bergen, Norway
[c] Institute of Marine Research, Austevoll Research station and Hjort Centre for Marine Ecosystem Dynamics, NO-5392 Storebø, Norway
[d] UniResearch AS, NO-5006 Bergen, Norway

ARTICLE INFO

Article history:
Received 11 March 2016
Received in revised form
23 June 2016
Accepted 27 June 2016
Available online 30 June 2016

Keywords:
Visual opsins
Rod
Cone
Nr2e3
Indirect development
Atlantic cod
Metamorphosis
RNA-Seq

ABSTRACT

Unlike in mammals, persistent postembryonic retinal growth is a characteristic feature of fish, which includes major remodeling events that affect all cell types including photoreceptors. Consequently, visual capabilities change during development, where retinal sensitivity to different wavelengths of light (photopic vision), -and to limited photons (scotopic vision) are central capabilities for survival. Differently from well-established model fish, Atlantic cod has a prolonged larval stage where only cone photoreceptors are present. Rods do not appear until juvenile transition (metamorphosis), a hallmark of indirect developing species. Previously we showed that whole gene families of *lws* (red-sensitive) and *sws1* (UV-sensitive) opsins have been lost in cod, while *rh2a* (green-sensitive) and *sws2* (blue-sensitive) genes have tandem duplicated. Here, we provide a comprehensive characterization of a two-step developing duplex retina in Atlantic cod. The study focuses on cone subtype dynamics and delayed rod neurogenesis and differentiation in all cod life stages. Using transcriptomic and histological approaches we show that different opsins disappear in a topographic manner during development where central to peripheral retina is a key axis of expressional change. Early cone differentiation was initiated in dorso-temporal retina different from previously described in fish. Rods first appeared during initiation of metamorphosis and expression of the nuclear receptor transcription factor *nr2e3-1*, suggest involvement in rod specification. The indirect developmental strategy thus allows for separate studies of cones and rods development, which in nature correlates with visual changes linked to habitat shifts. The clustering of key retinal genes according to life stage, suggests that Atlantic cod with its sequenced genome may be an important resource for identification of underlying factors required for development and function of photopic and scotopic vision.

1. Introduction

In contrast to the situation in mammals, a unique feature of the teleost eye is continued retinal growth and plasticity associated with postembryonic changes and development (Evans and Fernald, 1990). The two most extreme developmental programs that fish may follow are the indirect and direct development (Balon, 1985). Typical for the indirect developing species are the production of numerous progeny, where only a few survive into the specialized larval form (altricial strategy) (Balon, 1985). The direct developing fishes on the other hand, complete development prior to hatching and display a compression of the developmental time (embryonization), and loss of a true larval stage (Matsuda, 1987). When it comes to retina development, the most profound changes are seen in marine fish that follow an indirect developmental program. Marine fish larvae typically hatch with an undeveloped retina and undergo a lengthy pure-cone larval stage during which major body and retinal growth also take place (Balon, 1985). After a time that differs from species to species, the larva metamorphoses into a juvenile. This process affects the retina at several levels, including individual cell types and the expression of visual pigments, the production of new cell types and increased cellular interconnectivity (Evans and Fernald, 1990; Stenkamp, 2007).

The visual photopigment component opsin mediates

* Corresponding author.
[1] Present address: Sars International Centre for Marine Molecular Biology, NO-5008 Bergen, Norway

http://dx.doi.org/10.1016/j.ydbio.2016.06.041

absorption of light in both rods and cones. While rods responsible for dim-light vision express only rhodopsin (RH1), the four major classes of vertebrate cone opsins used for bright-light color vision are: Short wavelength-sensitive 1 and 2 (SWS1, SWS2), medium wavelength-sensitive (RH2), and long wavelength-sensitive (LWS) (Yokoyama, 2000). Cone opsins are categorized according to the pigment's peak sensitivity within the UV, blue, green and red regions of the electromagnetic spectrum, respectively (Yokoyama, 2000). Differential expression of visual opsins, together with change of chromophore types during ontogeny and spatially within the retina, occurs in both fish and mammals (Levine and MacNichol, 1982; Ahnelt and Kolb, 2000). However, the presence of multiple opsin paralog genes, commonly closely linked into tandem repeats in the genome, is, with a few exceptions (e.g. primate M/LWS) a characteristic feature of fish (Ibbotson et al., 1992; Rennison et al., 2012). These tandem-linked genes may be spatially or temporally regulated, and thus may tune sensitivity to light (Tsujimura et al., 2007).

In species such as zebrafish that have a direct development scheme, duplex retina formation (cones and rods) takes place in the embryo and prior to hatching (Raymond et al., 1995). However, in two-step retina development, the major remodeling is developmentally delayed and controlled by mechanisms that affect the identity of the expressed cone opsins, the ratio of cone to rod neurogenesis and the formation of regular cone mosaics (Evans and Browman, 2004). It is still unclear how these processes are regulated and to what extent the changes that occur during metamorphosis recapitulate the mechanisms that are active in the embryonic retina (Evans and Fernald, 1990). In zebrafish and goldfish, retinal neurogenesis is initiated asynchronously within all retinal cell layers, causing spreading out of fan-shaped waves of neurogenic differentiation that are complete during the larval phase (Raymond et al., 1995; Malicki, 2004; Neumann and Nuesslein-Volhard, 2000; Hu and Easter, 1999; Stenkamp et al., 1996; Schmitt and Dowling, 1996). As a result, both rods and cones follow a similar initial differentiation pattern in spite of originating in different stem cell populations; namely the inner nuclear layer (INL) Müller glia and the ciliary marginal zone (CMZ) multipotent lineage, respectively (Raymond et al., 1995; Stenkamp, 1996; Hitchcock and Kakuk-Atkins, 2004; Otteson et al., 2001). Although ventronasally initiated differentiation waves have been considered to be a general feature of teleosts (Stenkamp, 2007), there are some exceptions (Kitambi and Malicki, 2008; Cheng et al., 2007) that indicate alternative regulation of retinal stem cells.

Studies focusing on cone vs rod identity have taken a “candidate gene” expression approach in both fish and mammals where a number of factors, mainly transcription factors have been suggested to be either rod- or cone-specific (Stenkamp, 2007; Swaroop et al., 2010). The nuclear receptor subfamily 2, group E, member 3 (Nr2e3) is an orphan nuclear receptor which, together with the neural retina leucine zipper (Nrl) and cone-rod-homeobox (Crx), may both suppress cone genes and commit cells to a rod fate, and also serve as a co-activator of rod genes (Oh, 2008; Chen et al., 2005; Cheng, 2004). In zebrafish, however, the array of photoreceptor (PRC) transcription factors (TF), including Nr2e3, expressed by rod lineage cells is no different from the corresponding set expressed by cells destined to become cones, in that a truly rod-specific marker does not exist (Stenkamp, 2011). Hence, a two-step developing retina provides a unique system for the study of a pure-cone retina and subsequent rod neurogenesis, as these processes are separate in both time and developmental stage.

Atlantic cod follow an indirect path of ontogeny marked by metamorphosis (larvae-juvenile transition), in the course of which the larval pure-cone retina is transformed into a duplex retina in the juvenile by the development of the rods (Pedersen and Falk-Petersen, 1992; Tupper and Boutilier, 1995). Hence, vision changes from photopic to include scotopic vision concurrent with changes in life history. Combined with its sequenced and annotated genome and the possibility of segregating cone and rod neurogenesis temporally, we suggest that Atlantic cod could serve as an important comparative model species for studies of photoreceptor neurogenesis. We have previously showed that cod color vision is based on only blue-sensitive SWS2 (SWS2A and SWS2B) and green-sensitive RH2 (RH2A-1/2/3) opsins, where members of each opsin family are linked in tandem repeats, and different sets of opsins are expressed during the larval stage than in adults (Valen et al., 2014). In this study, we show that Atlantic cod provide a natural model system for photoreceptor specific studies, as development of cones and rods are temporally distinct events linked to developmental stages and metamorphic transition. The study shows that several retinal genes including the visual opsins are ontogenetically regulated. The cod retina thus allows for finer discrimination of photoreceptor specification and differentiation. We suggest that the use of comparative models with alternative developmental strategies could provide important answers and a more comprehensive and in-depth understanding of retinal development, plasticity and the functions of the underlying factors that regulate spatiotemporal gene expression.

2. Methods

2.1. Animals

All Atlantic cod material used in the current study was obtained from Austevoll Aquaculture Research Station, outside Bergen, Norway. The station has the required permission for catch and maintenance of Atlantic cod and a general permission to run as a Research Animal facility and to conduct experiments involving all developmental stages of fish (code 93) provided by the national Animal Care and Use Committee (Karlsen, 2015). Selected developmental stages from first-feeding to adulthood were sampled as described by Karlsen et al. (2015) (copepod group only). For information and permits regarding material used prior to first-feeding, see; Valen et al. (2014). All material was sampled in a light-adapted state, and sampled for gene expression analysis according to Valen et al. (2014). Since sampling of tissue was done post mortem, the fish was not considered as a research animal according to the Norwegian Animals in Research act. Hence further analysis on tissues obtained from these animals did not require any additional approval. Atlantic cod is not considered being an endangered species in Norway (national IUNC redlist: http://www.biodiversity.no/).

2.2. Atlantic cod staging

In the current study stages representing cod embryos and early larvae (prior to first feeding) will be referred to as days post fertilization (dpf; 1–18 dpf), from first feeding termed; days post hatching (dph) until end of metamorphosis, and thereafter; early juvenile and late juvenile (until maturation at ~1–2 year in captivity; then termed adult). In the current study embryos hatched at ~14–15 dpf, and started exogenous feeding at 18 dpf (~4 dph). The larval stages used include 4-, 11-, 22-, 29-, 37-, and 53 dph (previously termed 0–5 (Karlsen et al., 2015)), while the early juvenile stage correspond to 74- and 90 dph, and late juvenile (1-year). The metamorphosis period covers stages; 29-, 37-, and 53 dph, representing initial, mid and late metamorphosis, respectively. Standard length from 4 to 53 dph and early juvenile has previously been reported (Karlsen et al., 2015), and average total length of late juvenile cod (1-year) was 32 cm. In the current study

the 53 dph stage will also be termed early juvenile in the discussion.

2.3. RNA transcriptomics

The RNA extraction and sequencing was performed as previously described (Penglase et al., 2015). In short, total RNA from each biological triplicate was extracted from pools and cDNA sequencing libraries preparation and sequencing was performed by the Norwegian Sequencing Centre (NSC, Oslo, Norway) using the Illumina TruSeq RNA Sample Preparation Kit (Illumina Inc., San Diego, USA). The raw data has been deposited and can be found at The Sequence Read Archive (SRA) at NCBI (Accession ID: SRP056073). The RNA-Seq data was mapped to the coding sequences of the cod gene models (Star et al., 2011), using the Burrows-Wheeler aligner (Li and Durbin, 2009). Reads not mapping with at least 90% identity, or not mapping to exons, or with both pairs mapping on the same strand were removed. The reads were normalized by the total number of mapped sequences. Only genes with 10 reads or more in at least one of the samples were included for further analysis.

2.4. Heat maps

The transcriptomic profiles of 100 retinal genes were analyzed in the pure cone and duplex retina-life stages and included genes mainly involved in phototransduction pathway and eye/retina development and differentiation (transcription factors), but also genes linked to metamorphosis and growth. The gene selection was based on annotated function mostly in retina of other species (mainly zebrafish and mouse). To visualize expression patterns hierarchical clustering was performed using Euclidean distance of high level mean and variance normalized RNA expression data using J-express (Dysvik and Jonassen, 2001). See Supplementary Table S1 for normalized read counts of all genes displayed in the heatmap.

2.5. Quantitative real-time polymerase chain reaction (qPCR) of visual opsins

A qPCR was performed to confirm differentially expressed opsin genes (*sws2a*, *sws2b*, *rh2a-1*, *-2*, and *-3*, and *rh1*), including three reference genes (*ef1a, rpl4* and *ubiquitin*) in a total of five developmental stages (4-, 22-, 37- and 54 dph, and 1-year juvenile). To ensure enough RNA to analyze all genes, total RNA was extracted from whole larvae at 4 dph; including N=3 pools ten larvae each, and at 22 dph; including N=3 pools three larvae each. For the 37- and 54 dph stages, total RNA was extracted from dissected eyes, with N=3 pools of both right and left eye of 4 fish (one pool 8 eyes, and total N=24). For the 1-year cod, RNA from the right eye of 9 individuals was extracted. Hence the qPCR data from 4 and 22 dph is not directly comparable to the 37 and 54 dph, and 1-year stage. Total RNA was treated with RQ1 RNase-free DNase (Promega, Madison, WI, USA) and cDNA reversely transcribed using 700 ng total RNA and Oligo d($T_{15–18}$) in conjunction with the SuperScript III kit (Invitrogen, Carlsbad, CA, USA) as recommended by the manufactures and described in detail by Valen et al. (2014). A minus RT (no reverse-transcriptase enzyme) control of total RNA from all stages showed no signal for neither of the genes. RNA integrity was tested using Agilent 2100 Bioanalyzer (Agilent Technologies, Santa Clara, USA), with RNA integrity number (RIN) values above 8.3 confirming sufficient RNA quality (Fleige et al., 2006). Specific primers for all visual opsins were designed by placing primers in non-conserved areas (see Table 1 for; genebank accession number, primer info and product length). The qPCR assays were run on the CFX96™Real-Time System (Bio-Rad, Hercules, USA) with the following cycling conditions: 95 °C for 3 min, 40 cycles of; 95 °C for 15 s and 60 C for 1 min, and ended with 95 °C for 10 s, using relative expression of target to reference gene method and correcting for assay efficiency variation (Pfaffl, 2004). Each reaction was carried out on a volume of 12.5 μl using

Table 1
Primers used for qRT-PCR (qPCR) on Atlantic cod visual opsins, and for cloning and in situ hybridization (ISH) of *nr2e3-1* and *pcna*. Primers used for *rh1*, *nr2e3-1* and *pcna* RNA ISH probe included sequences of T3 (CATTAACCCTCACTAAAGGGAA) and T7 (TAATACGACTCACTATAGGG) promoter 5′ to the forward and reverse primers used for cloning (highlighted with *), respectively (according to Valen et al. (2014)).

Gene:	GenBank accession number:	Primers for qPCR and cloning/ISH probe*	Sequence (5′-3′):	Product size, base pairs (bp):
*Rh1**	AF385832	GM_RH1_Fw1	CCACACCGCAACCATGAACG	1233 bp
		GM_RH1_Rv1	GGGTCTGCTCTTCCTGCAAC	
Rh1	AF385832	GM_RH1_qPCR_Fw1	GAAGAAGAAGAAGATGAACACT	149 bp
		GM_RH1_qPCR_Rv1	ACAAACAGAAGCAGAAACAT	
Rh2a-1	AF385824	GM_RH2A-1_Fwd1	CTCTACCTGGACTCAATCAA	202 bp
		GM_RH2A-1_Rev1	ACAAACTCAAACACTTCATCT	
Rh2a-2	KJ572530	GM_RH2A-2_Fwd1	ATTCTTCTCCGTGCTACTT	97 bp
		GM_RH2-2A_Rev1	TGGATGCTATCAGGTGTC	
Rh2a-3	KJ572531	GM_RH2A-3_Fwd1	TGAGTGAGTGAGTGAATGT	105 bp
		GM_RH2A-3_Rev1	CCTGATGCTTAATGAATGGAT	
Sws2a	AF385822	GM_SWS2a__Fwd1	GTTGGCTGGAGTAGATACA	145 bp
		GM_SWS2a_Rev1	AGAGAATGGTGGCTAAGG	
Sws2b	KJ572532	GM_SWS2b_Fwd1	CCGTCATCTACATCCTACTAA	148 bp
		GM_SWS2b_Rev1	AATGCTTGTCTGAACTATGC	
*Nr2e3-1**	KT387747	GM_Nr2E3_F2*	GCTAACCTCCTGTGTGCTCC	646 bp
		GM_Nr2E3_R2*	CCTTGAAGCGGCTGAACACCTC	
*Pcna**	KC204826	GM_Nr2E3_F2*	TATCCACTGCTGTGTGATGCTG	1209 bp
		GM_Nr2E3_R2*	TTAAGGGCCGGTTTGATGACG	
Six7	KX173792	GM_Six7_F2*	AATGTTTCACCTGCCCATGTTC	532 bp
		GM_Six7_R2*	CTTGAACCAGTTGCCGACC	
Ef1a	EX721840	GM_EF1a_Fw1	CATCAACATCGTGGTCATT	96 bp
		GM_EF1a_Rv1	ATGGTTCTCTTGTCAATGC	
Rpl4	EX725958	GM_RPL4_Fw1	AATCGCCTGTATGAACCT	199 bp
		GM_RPL4_Rv1	AATCCTCTGAAGAACCTGAA	
Ubiquitin	EX735613	GM_Ubiq_Fw1	AGATTCAGGATAAGGAAGGAA	109 bp
		GM_Ubiq_Rv1	GACTCTTTCTGGATGTTGTAAT	

the iTaq™ universal SYBR® Green supermix (Bio-Rad). Melting curve analysis was performed on all genes (65 °C to 95 °C, with increment of 0.5 C for 5 s) that showed a single peak, indicating amplification of a single product (no signal was detected in the non-template control (NTC)). The gene expression values were normalized to an internal housekeeping gene; *ubiquitin*, ranked as the best out of three genes using the NormFinder algorithm (MDL, 2004, Denmark).

All statistical analyses were performed in Statistica 12.0. (StatSoft, Inc., Round Rock USA). A one-way ANOVA was performed to determine differentially expressed genes using stage as independent variable. In case of significant ANOVAs, Tukey-HSD post-hoc test was used to identify differences. Homogeneity of variances and normality of distributions were tested using Levene's test and Shapiro-Wilk test, respectively (Zar, 1996). As qPCR on the 4- and 20 dph stage was performed on whole larvae, and 37-, 53 dph and 1 year stage on dissected eyes; statistical analysis was separated for these groups.

2.6. In situ hybridization (ISH)

In the current study we used ISH RNA probes for cone opsins and the procedure previously described for both whole mount and sections (Valen et al., 2014), on embryonic [12–17 days post fertilization; ~60% hatched at 15 dpf], larval, and juvenile stages, and where the 4–54 dph represent the same material used for RNA-Seq. The synthesis of specific probes for *rh1*, *nr2e3-1*, *pcna* and *six7* was carried out in a similar procedure as for cone opsins, and additional details concerning gene accession number, primers and product length are described in Table 1. For fluorescent double-labeling ISH (FISH) of *sws2a-sws2b* and *nr2e3-rh1*, we followed the procedure previously described (Eilertsen et al., 2014). Fast Red (Roche Diagnostics, Mannheim, Germany) (for *sws2a, rh1*) and TSA™ Plus Fluorescein system (Perkin Elmer, Waltham, USA) (for *sws2b, nr2e3-1*) was used in combination. Enzymatic reactions with alkaline phosphatase (AP) linked to DIG-(Roche) (*sws2a, rh1*), and horseradish peroxidase (HRP) linked to fluorescein (Roche Diagnostics, Basel, Switzerland) (*sws2b, nr2e3-1*) was conjugated to RNA probes, respectively. After visualization of anti-DIG-AP probes with Fast Red, sections were blocked for 1 h in 2% Blocking reagent (Roche Diagnostics) in 2 × SCC before incubating with anti-fluorescein-POD and TSA visualization. A similar procedure was followed for cone mosaic studies (described below) where Fast Red-anti-DIG-AP was used on *sws2a* and TSA-anti-fluorescein-POD on *rh2a-1*. For additional information regarding antibodies, see; Eilertsen et al. (2014). All sections where mounted in ProLong® Gold Antifade Mountant with DAPI (ThermoFisher Scientific, Waltham, USA). Based on a z-stack of *sws2a-sws2b* images, a movie was prepared to better visualize co-localization of transcripts (see Supplementary Movie 1).

Supplementary material related to this article can be found online at http://dx.doi.org/10.1016/j.ydbio.2016.06.041.

2.7. TUNEL staining for apoptotic cells

In order to identify the presence of apoptotic cells related to plasticity of retinal photoreceptors, a TUNEL stain was performed on cryosections of 37 dph cod larvae. The stain was performed using the TACS® 2 TdT-DAB *In Situ* Apoptosis Detection Kit (Trevigen, Maryland, USA), following manufacturer's instructions. Careful analysis of cod did not show any sign of apoptosis at this stage, although apoptotic cells were detected in extra-retinal tissues including brain. Hence, the data from this analysis is not shown in the current manuscript.

3. Results

3.1. Establishment of photopic vision: initiation of cone differentiation

All opsin-expressing cones except RH2A-1 appeared by 13 dpf in a peripheral dorso-temporal area of retina (Fig. 1: A/B/C/D/E1 and -4). *Rh2a-1* expression was first detected at 15dpf in the same area, however extending farther towards the nasal and temporal areas of the retina (Fig. 1C2, C5). No expression of any of the genes was detected at 12dpf (data not shown), which is also confirmed by our previous real time-PCR at the same stage ((Valen, 2014); Suppl. Fig. S3). Differentiation of all cone types, except *rh2a-1*, then spread bi-directionally towards the nasal, ventral and central retina, eventually covering most regions of the retina (Fig. 1: A/B/C/D/E2, -3, -5 and -6). RH2A-1-cones showed a similar but delayed differentiation pattern, and were restricted to the dorso-temporal region at the time (17 dpf) at which RH2A-3/2 cones were dominating expression (Fig. 1C/D/E3 and C/D/E6).

3.2. Transformation of the pure-cone retina and life-stage transition

The tandem-organized *rh2* opsin genes showed the most dramatic change in expression (Fig. 2). The *rh2a*-2 and -3 opsins that dominated during early larval (15 dpf-11 dph) stages were shut off in the late juvenile during metamorphosis; first from the central, then dorsal and ventral retina (Fig. 2E1–F10). This was consistent with quantitative mRNA expression levels (Fig. 3). Concurrent with a drop in *rh2a-2/3* expression, the restricted dorsotemporally expressed *rh2a-1* in early larvae was extended ventrally to dominate all retinal regions during metamorphosis (Fig. 2D1–D10). The increase in *rh2a-1* expression cones was supported with quantitative *rh2a-1* levels (Fig. 3), which also showed that *rh2a-1* is the only *rh2* gene expressed in later juvenile stages (90 dph and 1 year juvenile) (Fig. 3A,B,D). The two *sws2* genes (Fig. 2A1/2–B10) were less regulated. However *sws2b* expression also disappeared, first from central, then the dorsal retina during metamorphosis (Fig. 2A2–J2). *Sws2b* expression was not detected by qPCR in the 1 year cod (Fig. 3D). The SWS2A cones appeared to be more regularly spaced during metamorphosis (Fig. 2A4, -5, -9, 10). Yet, a dramatic change into a strict mosaic pattern of *sws2a* expressing single cones, and *rh2a-1* expressing double cones was not detected during larvae-juvenile transformation (data not shown). A *sws2b-sws2a* expressional transition zone near the ventral CMZ was detected in larval and early juvenile stages (Fig. 2C1–10), where a region populated exclusively by SWS2B cones was found closest to the CMZ, and then by *sws2a* cones when moving from CMZ towards central retina (Fig. 2C1, C6–C10). In the 4 dph larvae some cones positioned in the *sws2b-sws2a* transition zone seemed to co-express *sws2a* and *sws2b* (Fig. 2C1, C6 and C7, and Supplementary Movie 1).

3.3. Development of scotopic vision: delayed rod neurogenesis and retina remodeling

Differentiated rods expressing *rh1* were first detected at the onset of metamorphosis (29 dph) in a few scattered cells, first in the dorsal, followed by the ventral retina (not in or close to CMZ) (Fig. 4A′, A1 and A4). This was consistent with quantitative *rh1* expression levels (Fig. 3). Differentiated rods then dramatically increased in number during mid-metamorphosis (37 dph), mostly in the dorsal, followed by ventral retina, but appeared less in the central retina (Fig. 4A2 and A5). In the early juvenile stage (53 dph), differentiated rods were found in all regions (Fig. 4A3 and A6), and high expression of *rh1* was sustained in the late juvenile stage (Fig. 3D4). Proliferating cells (*pcna* positive labeling)

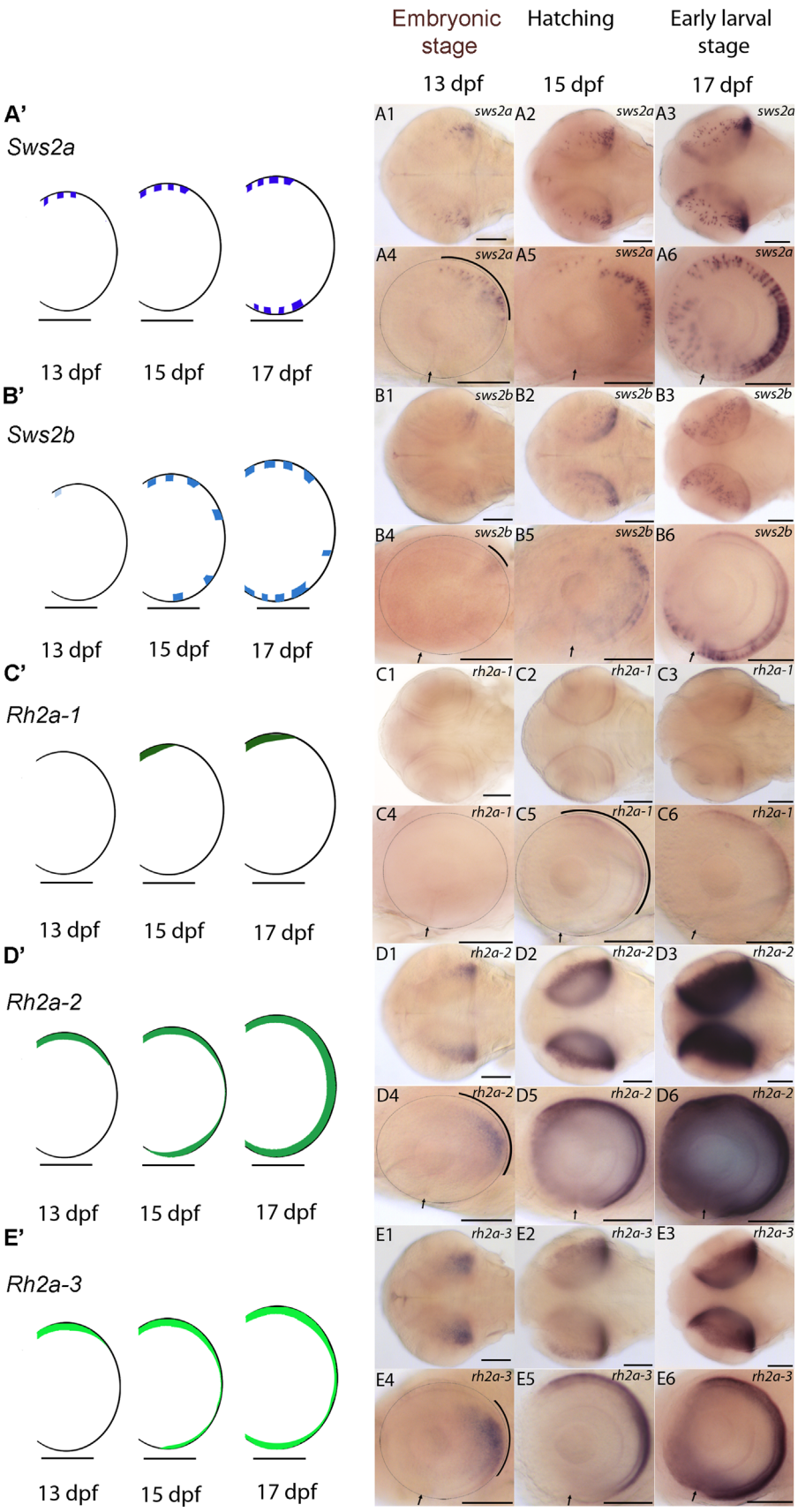

Fig. 1. Early initiation of cone photoreceptor differentiation in Atlantic cod. Whole mount in situ hybridization (right handside, A1-E6) using cone opsin subtype specific riboprobes were used to identify the spatio-temporal pattern of early cone differentiation in 13-, 15- and 17 dpf cod larvae (prior, during and post hatching, respectively). Left hand side represent a schematic summary of all differentiated cones (SWS2; A′ and B′, and RH2; C′, D′ and E′) from viewed in a left-eye transversal plane; peripheral to central (left to right), and dorsal-ventral retina (top to bottom) (A′–E′). Right hand side show expressed cone opsins in both dorsal view (A/B/C/D/E1–3) and lateral view (A/B/C/D/E4–6), and show that all cone opsins except *rh2a-1* is expressed at 13 dph in cones restricted to a peripheral dorsal-temporal region of retina, highlighted with a black curve in lateral view. Topographic location of *rh2a-1* expressing cones was first identified in 15 dph larvae (C2, C5), also in a dorsal-temporal region. Arrows in lateral view indicate location of embryonic fissure. Scale bar: 100 μm.

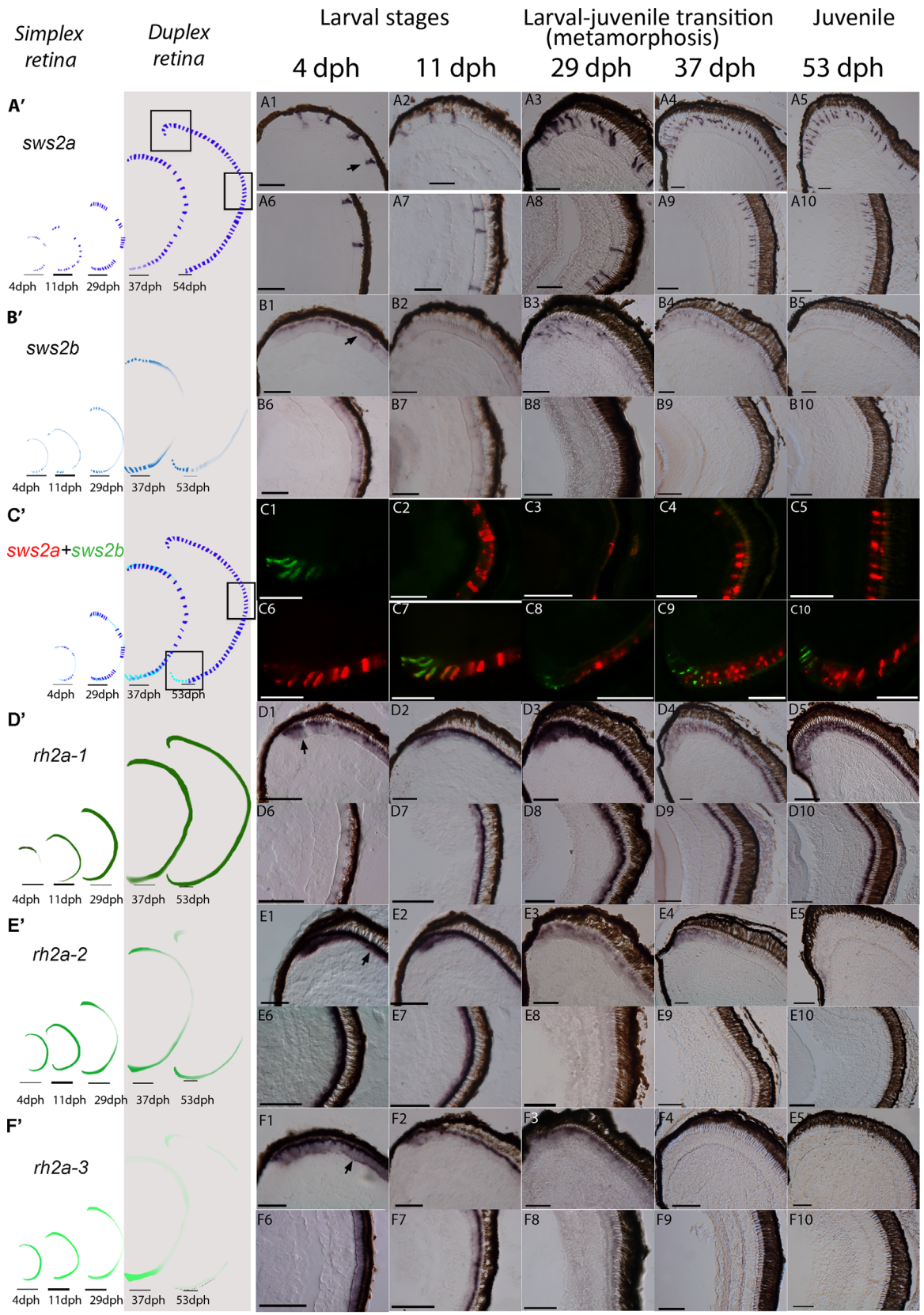

Fig. 2. Retinal transformation in cone opsins during postembryonic growth. *Left handside:* A schematic summary of sectional in situ hybridization (ISH) results of *sws2a* and *sws2b* (A′, B′), *sws2a-sws2b* (C′), and *rh2a-1*, *rh2a-2* and *rh2a-3* (D′, E′, F′) mRNA expression viewed in a transversal plane with size adjusted to respective developmental stages. Developmental stages with a duplex retina is marked with grey background, and black boxes on SWS2A in 53 dph indicate regions where ISH results are shown (dorsal and central retina, transversal) for all cone opsins on *right hand side* (A1–B10, and D1–F10) using specific DIG labelled riboprobes visualized with the alkaline phosphatase enzyme and chromogenic NBT/BCIP stain. Developmental stage is listed on top. Double-labeling fluorescent ISH (FISH) of *sws2a* and *sws2b* is shown schematically on left hand side with black boxes indicating central and ventral regions (C′) where FISH expression is shown on right hand side (C1–C10). *Sws2a* is visualized with Fast Red (red), and *sws2b* with TSA system (green), shown in separate channels in C1 (*sws2b*) and C6 (*sws2b*) and combined for 4 dph larvae (C2, C7), and combined for 29 dph (C3, C8), 37 dph (C4, C9) and 53 dph (C5, C10). Arrows illustrate ISH staining of mRNA. Scale bar: 100 μm (chromogenic visualization) and 50 μm (FISH-double labeling).

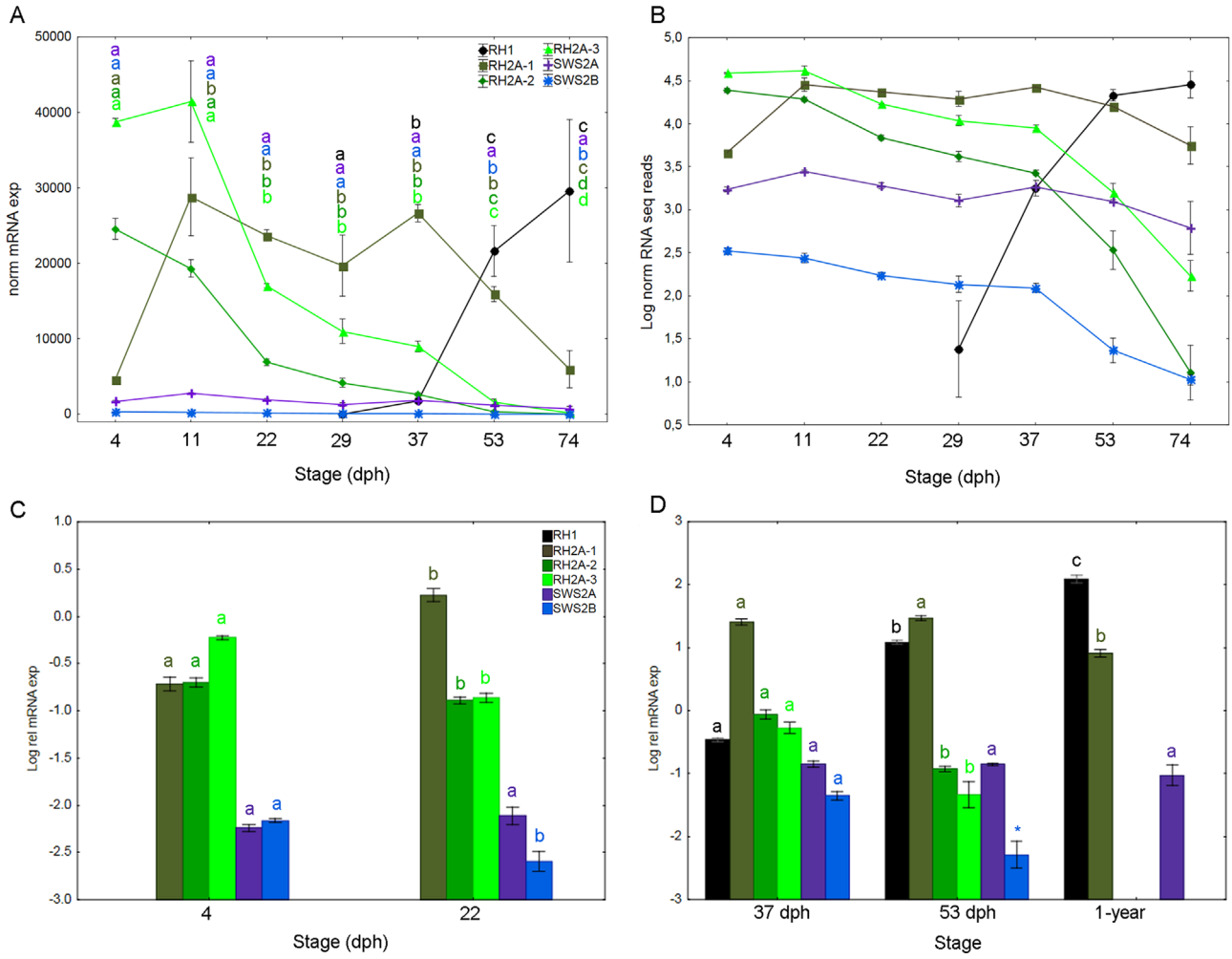

Fig. 3. Visual opsin dynamics during post-embryonic development, metamorphosis and in late juvenile Atlantic cod. A, B) RNA-Seq data on opsin expression shows the relative expression (see Methods section for details) of cone opsins (*y*-axis) in 7 developmental stages categorized in days post hatching (dpf); 4-, 11-, 22-, 29-, 37-, 53- and 74 dph (*x*-axis). During the end of the yolksac stage and when onset of exogenous feeding starts (4 dph larvae), all cone opsins are expressed, with the *rh2a-3* and *rh2a-2* subtypes being the two most expressed cone opsin genes. However, in the period from 10 dph to 30 dph, approaching onset of metamorphosis, expression of *rh2a-1* increases while *rh2a-3* and *rh2a-2* expression decreases. Coinciding with changes in *rh2a* expression profiles, is onset of *rh1*; *rhodopsin* in differentiating rods (30–45 dph), and initiation of cod metamorphosis. From 45 to 60dph *rh1* expression is dramatically increased as the larvae is transformed to a juvenile, and is the most expressed gene in the 90 dph juvenile. C, D) Confirmation of visual opsin dynamics was done with qRT-PCR on 4 selected developmental stages (4-, 20-, 37- and 53 dph), covering the metamorphosis period, in addition to late juvenile cod (~1year). The column representing sws2b in D) is noted with an * as 30% of the individuals had levels below qPCR quantifiable range. Gene specific primers were used for all visual opsins. The gene expression values were normalized to an internal housekeeping gene; ubiquitin ranked as best out of three genes using the NormFinder algorithm. For gene accession numbers; see Supplemental Table S1. Significant different expressed genes ($p < 0.05$) between stages is noted with different letters color coded according to gene description in A.

were mainly restricted to CMZ prior to rod differentiation (prior to 29 dph not shown). However, at onset of metamorphosis *pcna* expression was detected in inner nuclear layer (INL) and INL- outer nuclear layer (ONL) margin, some with fusiform shape (Fig. 4B′, B1 and B4). During mid-metamorphosis proliferating cells were also detected in basal regions of the dorsal and ventral ONL, and then mainly in INL as the central retina was approached (Fig. 4B2 and B5). The same pattern was seen in the early juvenile; however it was more extensive in ONL towards the central retina, and also more apically in ONL (Fig. 4B3 and B6).

3.4. Developmental profile of retinal genes including nr2e3-1 and six7 spatiotemporal expression

Retinal genes clustered into three main groups based on expression profile, representing genes with highest expression during the pure-cone stages: Cluster 1 (56 genes including *sws2a*, *sws2b*, *rh2a-2*, *rh2a-3 and six7*), retina transition phase: Cluster 2 (24 genes including *rh2a-1*), and a duplex-retina: Cluster 3 (20 genes including *rh1*), respectively (Fig. 5). *Rh1* appeared in Cluster 3 together with *nr2e3-1*. The highest number of genes is represented in Cluster 1 where 21 genes have annotated function in the phototransduction pathway, and 25 genes associated with transcriptional regulation. For additional information concerning gene molecular function based on gene ontology (GO) annotation and Ensemble no., see Fig. 5.

Retinal expression of the *nr2e3-1* gene was mainly detected in CMZ at onset of metamorphosis; however a few *nr2e3-1*-expressing cells were present in the INL-ONL margin in various regions (Fig. 4C′, C1 and C4). The low *nr2e3-1* expression level detected by ISH at 29 dph is consistent with the RNA seq temporal expression profile. During mid- and late metamorphosis, *nr2e3-1* displayed a similar spatiotemporal expression pattern to that of *rh1* (Fig. 4C2, C3, C5 and C6). Yet, a *rh1-nr2e3* double-labeling (mid-metamorphosis) detected cells that expressed only *nr2e3-1* in most dorsal retina, as well as in both basal and apical ONL (regions where rods

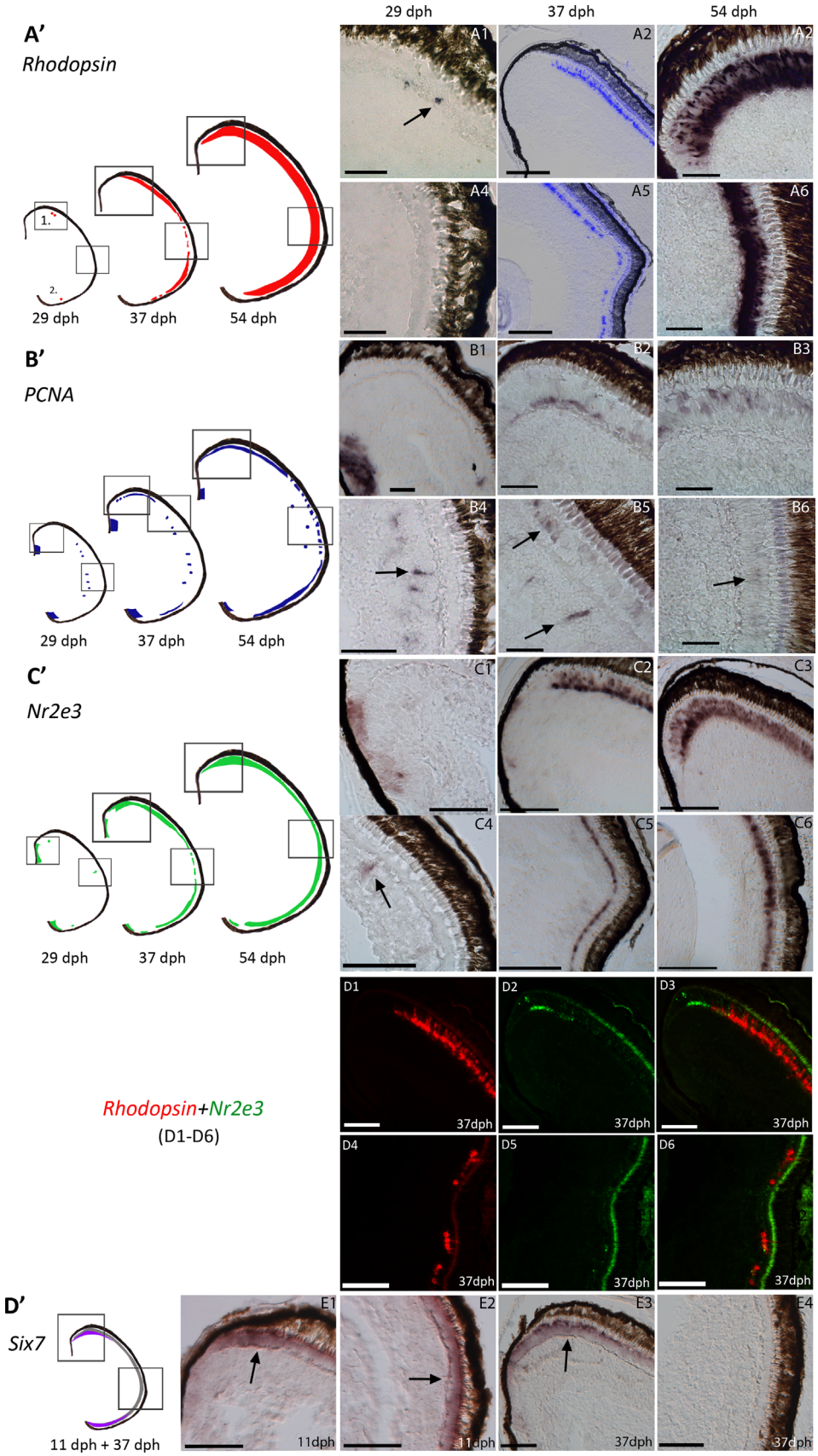

Fig. 4. Delayed rod neurogenesis and development of a duplex retina during Atlantic cod metamorphosis. *Left row*: Schematic summary of *rhodopsin* (*rh1*) (A′), *pcna* (B′), *nr2e3-1* (C′), and *six7* (D′) mRNA expression in Atlantic cod during stages around metamorphosis (29-, 37-, and 54 dph) and at 11 dpf (for *six7*). Black boxes indicate retinal region (dorsal and central) where in situ hybridization (ISH) is shown for the same stages for *rh1* (A1–A6), *pcna* (B1–B6), *nr2e3-1* (C1–C6) and *six7* (E1–E4), using chromogenic (NBT-BCIP) stain for all but A2 and A5; which were visualized with Fast Red and given a blue pseudocolor. For *six7* the schematic representation of expression (D′) is shown as an overlap of the 11 dph stage (shown in grey) and the 37 dph stage (shown in purple). For *rh1* the temporal sequence and location of initial appearance of differentiated rods are indicated with numbers 1. (first expressed) and 2. (subsequent expression). A double labeling fluorescent ISH was performed on *rh1* (Fast Red-red) and *nr2e3-1* (TSA-green) during mid metamorphosis (37 dph) (D1–D6), where separate channels are shown for *rh1* (Fast Red) in D1 and D4, and *nr2e3-1* (TSA) in D2 and D5, and overlay in D3 and D6; in dorsal and in proximity to central retina, respectively. Arrows* indicate stained mRNA expression, while the weak purple color in some outer segments most likely is caused by background stain. Scale bar: 100 μm (A1–C6) and 50 μm (D1–E4).* The arrow in 4B6 likely points to low expression of *pcna* in the photoreceptor layer.

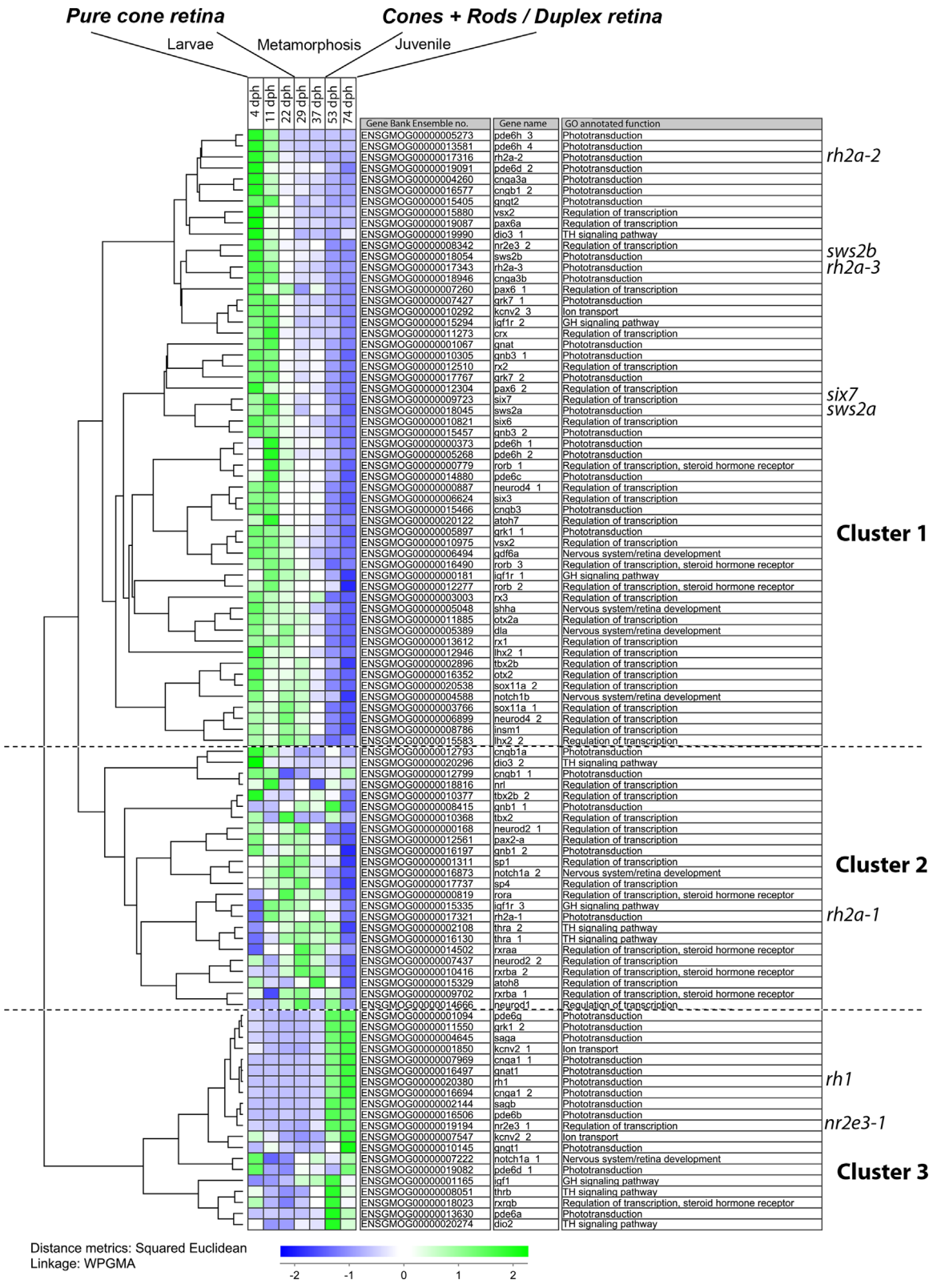

Fig. 5. Transcriptomic profile of retinal genes in stages of pure cone-, transforming, and duplex retina. Heat map from hierarchical clustering using Euclidean distance of high level mean and variance normalized RNA-Seq expression data on 100 retinal genes (see Section 2). Green color illustrates peak gene expression, while blue illustrates lowest level of expression. To distinguish between paralogs we have added a sequential number to the gene name; Swiss-prot ID (i.e. pde6d_1 and pde6d_2). See Supplementary Table S1 for normalized RNA-Seq counts of all genes displayed in the heatmap.

had yet to be differentiated) (Fig. 4D1–D4). Expression of the *six7* gene was detected in ONL throughout retina in the 11 dph larvae, however was lost from the central retina during the 37 dph stage (Fig. 4D′, E1–E4). The high expression of *six7* detected in retina during early larval stages, and lower expression in later developmental stages is consistent with the Cluster 1 expression profile (Fig. 5).

4. Discussion

4.1. Summary of main findings

Our main findings in this study of a retina with stepwise and separate life-stage development of photopic and scotopic vision are as follows: 1) The differentiation and maintenance of specific cones change with development and involve a topographic gradient where CMZ appears to retain the "larval program" during juvenile transformation. 2) Development of scotopic vision is concurrent with life-stage transition and loss of cone subtypes, where differentiating rods follow a gradient with increased abundance in distinct retinal regions. 3) Transcriptomic analysis of indirect developing species provides an efficient tool for the characterization of factors required for photopic and scotopic vision development (and function). In the latter case, both the *nr2e3-1* gene along with *rh-1*, and *six7* along with cone opsin paralogs, are clearly regulated according to life-stage transition.

4.2. Early establishment of photopic vision

The embryonic neurogenic differentiation of cones is an attractive process, as the patterning of these cones is different than that of the peripheral CMZ differentiated cones of the growing retina of later developmental stages. In cod, cones first exit the cell cycle and differentiate in the dorsal retina, which is the opposite of the ventral initiation in the cyprinids zebrafish and goldfish (Raymond et al., 1995; Hu and Easter, 1999; Stenkamp et al., 1996; Schmitt and Dowling, 1999). Salmon, on the other hand, undergo centro-temporal initiation of some cone types that may represent a more evolutionarily conserved differentiation pattern than the well-established ventronasal "neurogenic initiation centre" of cyprinids (Cheng et al., 2007). It has been suggested that embryonic waves of neurogenesis reflect an earlier patterning gradient, laid down when the optic primordium was a solid paddle-shaped mass (Li et al., 2000), where both *atonal* and *shh* genes have been shown to play a role in neurogenesis (Neumann and Nuesslein-Volhard, 2000; Masai et al., 2000; Stenkamp et al., 2000). Whether these patterning genes display an alternative gradient in cod that mainly affects cones is currently unknown, as is the functional significance related to development of visual function. It should be noted that cones cannot gather visual information before all neuronal classes (except rods) have established synaptic connections, and features such as photoreceptor outer segments and long ganglion processes that extend to the midbrain (Hu and Easter, 1999; Young, 1985; Holt et al., 1988; Attardi and Sperry, 1963; Burrill and Easter, 1995; Lemke and Reber, 2005).

4.3. Transformation of a pure-cone retina: opsin plasticity and cone re-organization

The continued expression of all cone opsins in proximity to the CMZ area during metamorphosis suggests the maintenance of a larval CMZ cone identity program. All cone opsins are expressed in ventral CMZ in the early juvenile, although *sws2b* expressing cones was not detected in dorsal retina at this stage. Together with the weak expression of *rh2a-3* in dorsal retina of the 37 dph cod, it may suggest that there is also a dorsal-ventral CMZ gradient present. The major spatiotemporal regulation of cone subtypes in cod, particularly of those that express *rh2* opsins (also *sws2b*), further suggests that there are gene and/or cell-type regulatory mechanisms that act differentially on retinal regions during development. Interestingly, the loss of *rh2a-2/3* and *sws2b* expression from the central retina suggests the involvement of other mechanisms than CMZ inhibition of differentiation (control), a notion that is supported by the prolonged expression of opsins in CMZ region. Alternatively, the central retina may lack expressional activation signals that may still be present in the peripheral retina (or is under expressional inhibition). This is in contrast to *rh2a-1*, where expression is not spatiotemporally regulated once it has been expressed in all retinal regions in the larva.

Interestingly, a similar *rh2a-2/3* CMZ to central retina gradient, was also observed for the *six7* homeobox transcription factor. Recent studies have suggested a dual role for six7 in photoreceptor regulation that involves both control of rod number, and survival of green sensitive cone precursors (Ogawa et al., 2015; Sotolongo-Lopez et al., 2016). Although these studies suggest that Six7 is required for zebrafish *rh2* expression and green cone survival, our expression data may point towards a differential role of six7 in cod related to *rh2* paralog. This is supported by the overlapping expression pattern of *six7* and *rh2a-2/3* in early larval stages, and during metamorphosis (in proximity to CMZ). Yet, cod *rh2a-1* expression pattern is not similar to *six7*, neither in larvae nor during juvenile transformation. Furthermore, in agreement with an increase in zebrafish rod number caused by *six7* knockdown, the decrease in *six7* expression during cod metamorphosis coincides with appearance of rods (Sotolongo-Lopez et al., 2016). Altogether, future studies are needed to unravel the exact role of six7 in photoreceptor regulation in cod.

In zebrafish spatiotemporal regulation of tandem-linked cone opsins is achieved through shared locus-control regions (lcr) acting on downstream promotor activation (Tsujimura et al., 2015; Takechi and Kawamura, 2005; Chinen et al., 2003). Duplicated genes may thus use shared regulatory regions in a competitive manner in order to obtain differential gene expression, and this competition may be under developmental control. *Rh2*, *lws* and *sws2* genes have all been shown to have binding sites for transcription factors involved in retinal differentiation in zebrafish (Tsujimura et al., 2007, 2010; Takechi et al., 2008; Chen et al., 1997; Furukawa et al., 1997). However, it remains to be shown whether the same mechanism operates on cod cone opsins. It should be noted that there does not seem to be an obvious link between the syntenic organization of cod rh2 genes, and the order of expressional changes observed (Valen et al., 2014). Nevertheless, the delayed onset and continued expression of cod *rh2a-1*, combined with peripheral expression of *rh2a-2* and *rh2a-3*, does indicate at least two different developmental modes of expressional control that may involve *six7*.

The retention through metamorphosis of SWS2B expressing cones in the ventral retina near to the CMZ, suggests the presence of SWS2B-differentiation signals in this region. However, cones positioned slightly more centrally (and older) express both *sws2a* and *sws2b*, followed by cones that express only *sws2a* in more central and dorsal regions. This may suggests that these cones may transition from one fate to another; depending on time of birth and retinal position, and also that the larval activation of SWS2B is maintained in the ventral CMZ. Contrary to previous notions of a single visual pigment/opsin per photoreceptor (Mazzoni et al., 2004), several studies have reported co-expression of multiple opsins (Szél et al., 2000; Arikawa et al., 2003; Dalton et al., 2014; Isayama et al., 2014). In salmonids, opsin co-expression is a transient event related to a thyroid hormone-induced switch from UV- to blue-sensitive opsin in single cones during metamorphosis,

probably related to change in life style and prey preference (Cheng and Flamarique, 2007; Flamarique, 2013). Also in mammals, opsin co-expression has been reported in several studies (Hunt and Peichl, 2014). In cichlids, double-cones co-express *rh2* and *lws*, related to sensitivity tuning within specific retinal regions, which is thought to improve the perception of the background (Dalton et al., 2014). It has also been suggested that the expression of multiple *sws2* paralogs differentially tunes the retina to either violet or blue wavelengths, although the mechanisms by which this might take place is not known (Carleton et al., 2008). Although we do not have spectral absorbance data on the cod opsin SWS2B subtype, phylogeny places the cod SWS2b type among the violet-sensitive SWS2 opsin branch of other species (Valen et al., 2014). Whether the expression of multiple opsin subtypes in ventral retina is a consequence of expressional regulation, or/and has a functional role related to habitat shift during larvae-juvenile transformation is unknown.

The loss of *rh2a-2* and *rh2a-3* expression further supports our previous findings that the adult mosaic pattern is based on *sws2a* expressing single cones, and *rh2a-1* expressing double cones (Valen et al., 2014). Although the sws2a expressing single cones appeared more regularly during the time of rod differentiation, future studies are needed to characterize the exact morphometrics of cone mosaic (re)organization in cod. A reorganization of retina during metamorphosis, including fusion of single cones into double cones, and appearance of rods, has previously been shown in winter flounder (Evans and Fernald, 1993). In zebrafish the larval retina is retained within the adult retina and does not reorganize to form the adult pattern of regular rows (Allison et al., 2010). However, the loss of larval expressed *rh2a-2/3* from the central retina in cod, combined with continued CMZ expression, suggests the presence of more plastic mechanisms than the mere retention of the larval cone structure and generation of mosaics from post-larval CMZ growth. It has been suggested that processes as different as apoptosis, cell movement and lateral cell induction are involved (Allison et al., 2010). Yet, no signs of apoptotic cells were detected during cod metamorphosis (37 dph), a time when rh2a-2/rh2a-3 expression is disappearing, suggesting that loss of cone subtypes through apoptosis is not a major mechanism in cod. However, we also hypothesize that spatial transition of cone fate through *rh2a* opsin switch may represent a mechanism involved in establishment of the adult cone pattern. All in all, the re-organization of the cod retina into the adult structure probably includes both the CMZ and the central retinal regulation of cones. Interestingly, both UV and red-sensitive LWS cones have been suggested to play guiding roles in cone mosaic organization of model fish (Wan and Stenkamp, 2000; Raymond, 2014; Stenkamp and Cameron, 2002), However this raises the question of how identity repetition is achieved in a retina that completely lacks *sws1* and *lws* genes.

4.4. Metamorphic development of scotopic vision: rod neurogenesis

The delayed appearance of rods in cod at the onset of larval-juvenile transition follows a two-step development of retina that involves developmental upregulation of cell proliferation in the INL and INL-ONL margin. The fusiform cell shape of some proliferating cells suggests that these are Müller glia-derived rod precursors (Raymond and Rivlin, 1987; Julian et al., 1998). Although the Müller glia rod-lineage is different from the stem-cell path of cones, newly differentiated rods first appear in dorsal retina, which subsequently contains the highest abundance of rods (expressing rhodopsin). This suggests a regional difference in signals leading to rhodopsin activation, yet it remains speculative at the moment whether this may be linked to the embryonic dorsal cone opsin activation. However, as rod cells differentiate in more randomly distributed spots and also in other retinal areas (ventral), rather than spreading from a confined area as do cones, the underlying patterning of rod neurogenesis is probably different. Early studies in zebrafish showed that expression of the rhodopsin gene was an early marker of differentiated cells, and expression was initiated in post-mitotic rod progenitor cells (Knight and Raymond, 1990). Hence the observed rhodopsin expression pattern likely reflects the pattern of rod progenitor cells that have undergone terminal mitosis, and areas without expression may represent continuously dividing rod progenitors.

The detection of secondary differentiated rods in the ventral retina (a pattern maintained through metamorphosis), may support a model of two spatially distinct rod-initiation domains, as suggested in medaka (Kitambi and Malicki, 2008), rather than the single ventral rod domain of cyprinids. Which domain is of most ancient origin is not known, and in salmonids rods follow a similar pattern to that of cones, which spread from the centro-temporal retina (Cheng et al., 2007). During the later stages of cod metamorphosis recognized by a rapid increase in rods, proliferative cells were found mainly in the ONL, in accordance with rod precursors dividing faster in the ONL than the INL (Otteson et al., 2001; Julian et al., 1998). Rod production has been shown to be under IGF control that regulates body growth, so that the precursor proliferation and regulation of rods are slowing in species with a well-defined period of body growth (e.g. zebrafish), unlike in those characterized by continued growth (cod) (Marcus et al., 1999). The developmental upregulation of cell proliferation during rod genesis may have parallels in regeneration processes or normal periods of rapid growth in other teleosts (Stenkamp, 2011; Cid et al., 2013; Faillace et al., 2002). Indirectly developing retinas might therefore provide a valuable model for the role of factors and pathways involved in rod cell activation and stem cell regulation in general.

4.5. Nr2e3-1 expression pattern is spatiotemporally linked to rod differentiation and metamorphosis

The similar spatiotemporal patterns of expression of *nr2e3-1* and *rhodopsin* during metamorphosis in cod suggest that Nr2e3 have a role in rod specification, as has been shown in zebrafish and mammals (Cheng et al., 2004; Nelson et al., 2008), although it follows a step-wise mode of regulation. In cod, *nr2e3-1* seems to precede the expression of rhodopsin that probably represents cells just prior to rod differentiation, as has been observed in zebrafish and mice (Chen et al., 2005; Kitambi and Hauptmann, 2007). Pre-metamorphic expression of *nr2e3-1* is restricted to CMZ, and may suggest a different role prior to rod genesis, a role that could be related to cone opsin regulation (Chen et al., 2005), although this remains to be demonstrated. Although the mechanisms that regulate rod fate vs cones is still somewhat unclear, Crx has been shown to bind to the conserved *otx* sequence in the zebrafish rod opsin promoter (Kawamura et al., 2005). A temporal hierarchy of rod PRC transcriptional control with Crx and Nrl above Nr2e3 has been suggested as a model (Peng et al., 2005). Whether and how the cod rod opsin promoter is regulated by Nr2e3 and is combined with other factors remains to be shown. Interestingly, we found that the cluster of genes that includes *rhodopsin* and *nr2e3-1* also includes the *kcnv2* gene that has been shown to be under the control of both Crx and Nrl in humans (Aslanidis et al., 2014). Furthermore, given that retinal transformation is linked to metamorphosis, thyroid hormone (TH) is probably a key upstream signaling factor that has been shown to influence cone subtypes and opsin expression in fish and mammals (Applebury et al., 2007; Cheng et al., 2009; Ng et al., 2001; Temple et al., 2008). In mice, the presence of the thyroid hormone receptor (TRb2) plays a role in both the specification of cone subtypes and spatial repression

that involves chromatin remodeling and permanently gene silencing in differentiated cones (Ng et al., 2001). However, the role of TH in rod neurogenesis (Nr2e3-Crx-Nrl) pathways remains to be identified.

In the current study we have provided a comprehensive and detailed analysis of photoreceptor differentiation in a species that follows a step-wise development of duplex retina. We have shown that the pure-cone retina of larval cod allows for specific studies of cones and opsin expression. These findings may provide a valuable basis for future studies involving identification and isolation of factors involved in the photoreceptor-specific pathway, and also in cone subset determination. Our identification and analysis of *nr2e3-1*, suggest involvement in rod specification linked to metamorphosis. Our study thus shows that *nr2e3-1* is regulated according to life-stage transition. The clustering of several key retinal genes according to life stage, exemplifies the power of cod retina as a comparative model system. Yet, functional analysis of these candidates in cod is challenged by long generation time and season restricted material, among others. However, when combined with established fish models, the benefits of a step-wise developing retina could potentially involve detection of key factors and gene regulatory hierarchies, which have previously been undetected.

Altogether, the stepwise development of cod retina reflects a life-stage specific regulation of photoreceptor pathways, which are a key element of a lifelong plastic, yet functional retina. The duplex retina of adult cod is capable of both color discrimination and high-sensitivity dim-light vision, which is a prerequisite for complex visual-guided behaviors essential for survival in a fluctuating light environment.

Acknowledgements

The authors thank Rita Karlsen for technical assistance on the qPCR on visual opsins and cloning of the *nr2e3-1* gene. We also thank the staff at Austevoll marine research station (Institute of Marine Research) for donation of high quality cod eggs. The current study was funded by the Norwegian Research Council, Norway in project CODE (#199482) and by University of Bergen, Norway through a PhD position.

Appendix A. Supplementary material

Supplementary data associated with this article can be found in the online version at http://dx.doi.org/10.1016/j.ydbio.2016.06.041.

References

Ahnelt, P.K., Kolb, H., 2000. The mammalian photoreceptor mosaic-adaptive design. Prog. Retin. Eye Res. 19 (6), 711–777.
Allison, W.T., et al., 2010. Ontogeny of cone photoreceptor mosaics in zebrafish. J. Comp. Neurol. 518 (20), 4182–4195.
Applebury, M., et al., 2007. Transient expression of thyroid hormone nuclear receptor TRβ2 sets S opsin patterning during cone photoreceptor genesis. Dev. Dyn. 236 (5), 1203–1212.
Arikawa, K., et al., 2003. Coexpression of two visual pigments in a photoreceptor causes an abnormally broad spectral sensitivity in the eye of the butterfly *Papilio xuthus*. J. Neurosci. 23 (11), 4527–4532.
Aslanidis, A., et al., 2014. RETINA-specific expression of Kcnv2 Is controlled by Cone-Rod Homeobox (Crx) and Neural Retina Leucine Zipper (Nrl). In: Ash, J.D., et al. (Eds.), Retinal Degenerative Diseases. Springer, New York, pp. 31–41.
Attardi, D.G., Sperry, R., 1963. Preferential selection of central pathways by regenerating optic fibers. Exp. Neurol. 7 (1), 46–64.
Balon, E.K., 1985. Early life histories of fishes: new developmental, ecological, and evolutionary perspectives. In: Balon, E.K. (Ed.), 1 edition ed. Development in EBF vol. 5. Dr. W. Junk Publishers, Dordrecht, Netherlands, p. 280.
Burrill, J.D., Easter, S., 1995. The first retinal axons and their microenvironment in zebrafish: cryptic pioneers and the pretract. J. Neurosci. 15 (4), 2935–2947.
Carleton, K.L., et al., 2008. Visual sensitivities tuned by heterochronic shifts in opsin gene expression. BMC Biol. 6 (1), 22.
Chen, J., Rattner, A., Nathans, J., 2005. The rod photoreceptor-specific nuclear receptor Nr2e3 represses transcription of multiple cone-specific genes. J. Neurosci. 25 (1), 118–129.
Chen, S., et al., 1997. Crx, a novel Otx-like paired-homeodomain protein, binds to and transactivates photoreceptor cell-specific genes. Neuron 19 (5), 1017–1030.
Cheng, C.L., Flamarique, I.N., 2007. Chromatic organization of cone photoreceptors in the retina of rainbow trout: single cones irreversibly switch from UV (SWS1) to blue (SWS2) light sensitive opsin during natural development. J. Exp. Biol. 210 (23), 4123–4135.
Cheng, C.L., Gan, K.J., Flamarique, I.N., 2007. The ultraviolet opsin is the first opsin expressed during retinal development of salmonid fishes. Investig. Ophthalmol. Vis. Sci. 48 (2), 866–873.
Cheng, C.L., Gan, K.J., Flamarique, I.N., 2009. Thyroid hormone induces a time-dependent opsin switch in the retina of salmonid fishes. Investig. Ophthalmol. Vis. Sci. 50 (6), 3024–3032.
Cheng, H., et al., 2004. Photoreceptor-specific nuclear receptor NR2E3 functions as a transcriptional activator in rod photoreceptors. Hum. Mol. Genet. 13 (15), 1563–1575.
Chinen, A., et al., 2003. Gene duplication and spectral diversification of cone visual pigments of zebrafish. Genetics 163 (2), 663–675.
Cid, P., et al., 2013. Analysis of the morphogenesis and cell proliferation in the retina of a pleuronectiform fish, the turbot Psetta maxima (Pleuronectiformes: Teleostei). Microsc. Res. Tech. 76 (6), 588–597.
Dalton, B.E., et al., 2014. Spectral tuning by opsin coexpression in retinal regions that view different parts of the visual field. Proc. R. Soc. B – Biol. Sci. 281 (1797), 9.
Dysvik, B., Jonassen, I., 2001. J-Express: exploring gene expression data using Java. Bioinformatics 17 (4), 369–370.
Eilertsen, M., et al., 2014. Exorhodopsin and melanopsin systems in the pineal complex and brain at early developmental stages of Atlantic halibut (*Hippoglossus hippoglossus*). J. Comp. Neurol. 522 (18), 4003–4022.
Evans, B.I., Fernald, R.D., 1990. Metamorphosis and fish vision. J. Neurobiol. 21 (7), 1037–1052.
Evans, B.I., Fernald, R.D., 1993. Retinal transformation at metamorphosis in the winter flounder (Pseudopleuronectes-americanus). Vis. Neurosci. 10 (6), 1055–1064.
Evans, B.I., Browman, H.I., 2004. Variation in the development of the fish retina. In: Govoni, J.J. (Ed.), The Development of Form and Function in Fishes and the Question of Larval Adaptation. American Fisheries Society USA, Bathesda, USA, pp. 145–166.
Faillace, M.P., Julian, D., Korenbrot, J.I., 2002. Mitotic activation of proliferative cells in the inner nuclear layer of the mature fish retina: regulatory signals and molecular markers. J. Comp. Neurol. 451 (2), 127–141.
Flamarique, I.N., 2013. Opsin switch reveals function of the ultraviolet cone in fish foraging. Proc. R. Soc. Lond. B: Biol. Sci. 280 (1752).
Fleige, S., et al., 2006. Comparison of relative mRNA quantification models and the impact of RNA integrity in quantitative real-time RT-PCR. Biotechnol. Lett. 28 (19), 1601–1613.
Furukawa, T., Morrow, E.M., Cepko, C.L., 1997. Crx, a novel otx-like homeobox gene, shows photoreceptor-specific expression and regulates photoreceptor differentiation. Cell 91 (4), 531–541.
Hitchcock, P., Kakuk-Atkins, L., 2004. The basic helix-loop-helix transcription factor neuroD is expressed in the rod lineage of the teleost retina. J. Comp. Neurol. 477 (1), 108–117.
Holt, C.E., et al., 1988. Cellular determination in the Xenopus retina is independent of lineage and birth date. Neuron 1 (1), 15–26.
Hu, M., Easter, S.S., 1999. Retinal neurogenesis: the formation of the initial central patch of postmitotic cells. Dev. Biol. 207 (2), 309–321.
Hunt, D.M., Peichl, L., 2014. S cones: evolution, retinal distribution, development, and spectral sensitivity. Vis. Neurosci. 31 (2), 115–138.
Ibbotson, R.E., et al., 1992. Sequence divergence and copy number of the middle- and long-wave photopigment genes in old world monkeys. Proc. R. Soc. Lond. B: Biol. Sci. 247 (1319), 145–154.
Isayama, T., et al., 2014. Coexpression of three opsins in cone photoreceptors of the salamander *Ambystoma tigrinum*. J. Comp. Neurol. 522 (10), 2249–2265.
Julian, D., Ennis, K., Korenbrot, J.I., 1998. Birth and fate of proliferative cells in the inner nuclear layer of the mature fish retina. J. Comp. Neurol. 394 (3), 271–282.
Karlsen, Ø., et al., 2015. Copepods enhance nutritional status, growth and development in Atlantic cod (*Gadus morhua* L.) larvae—can we identify the underlying factors? PeerJ, 3, p. e902.
Kawamura, S., et al., 2005. Evolutionarily conserved and divergent regulatory sequences in the fish rod opsin promoter. Comp. Biochem. Physiol. B – Biochem. Mol. Biol. 141 (4), 391–399.
Kitambi, S., Malicki, J., 2008. Spatiotemporal features of neurogenesis in the retina of medaka, *Oryzias latipes*. Dev. Dyn. 237 (12), 3870–3881.
Kitambi, S.S., Hauptmann, G., 2007. The zebrafish orphan nuclear receptor genes nr2e1 and nr2e3 are expressed in developing eye and forebrain. Gene Expr. Patterns 7 (4), 521–528.
Knight, J.K., Raymond, P.A., 1990. Time course of opsin expression in developing rod photoreceptors. Development 110 (4), 1115–1120.
Lemke, G., Reber, M., 2005. Retinotectal mapping: new insights from molecular genetics. Annu. Rev. Cell Dev. Biol. 21, 551–580.
Levine, J.S., MacNichol, E.F., 1982. Color vision in fishes. Sci. Am. 246 (2), 140–149.

Li, H., Durbin, R., 2009. Fast and accurate short read alignment with Burrows-Wheeler transform. Bioinformatics 25 (14), 1754–1760.
Li, Z., Joseph, N.M., Easter, S.S., 2000. The morphogenesis of the zebrafish eye, including a fate map of the optic vesicle. Dev. Dyn. 218 (1), 175–188.
Malicki, J., 2004. Cell fate decisions and patterning in the vertebrate retina: the importance of timing, asymmetry, polarity and waves. Curr. Opin. Neurobiol. 14 (1), 15–21.
Marcus, R.C., Delaney, C.L., Easter, S.S., 1999. Neurogenesis in the visual system of embryonic and adult zebrafish (*Danio rerio*). Vis. Neurosci. 16 (03), 417–424.
Masai, I., et al., 2000. Midline signals regulate retinal neurogenesis in zebrafish. Neuron 27 (2), 251–263.
Matsuda, R., 1987. Animal Evolution in Changing Environments: With Special Reference to Abnormal Metamorphosis. Wiley, New York.
Mazzoni, E.O., Desplan, C., Çelik, A., 2004. 'One Receptor' rules in sensory neurons. Dev. Neurosci. 26 (5–6), 388–395.
Nelson, S.M., et al., 2008. The developmental sequence of gene expression within the rod photoreceptor lineage in embryonic zebrafish. Dev. Dyn. 237 (10), 2903–2917.
Neumann, C.J., Nuesslein-Volhard, C., 2000. Patterning of the zebrafish retina by a wave of sonic hedgehog activity. Science 289 (5487), 2137–2139.
Ng, L., et al., 2001. A thyroid hormone receptor that is required for the development of green cone photoreceptors. Nat. Genet. 27 (1), 94–98.
Ogawa, Y., et al., Homeobox Transcription Factor six7 Governs Expression of Green Opsin Genes in Zebrafish, vol. 282, 2015.
Oh, E.C., et al., 2008. Rod differentiation factor NRL activates the expression of nuclear receptor NR2E3 to suppress the development of cone photoreceptors. Brain Res. 1236, 16–29.
Otteson, D.C., D'Costa, A.R., Hitchcock, P.F., 2001. Putative stem cells and the lineage of rod photoreceptors in the mature retina of the goldfish. Dev. Biol. 232 (1), 62–76.
Pedersen, T., Falk-Petersen, I., 1992. Morphological changes during metamorphosis in cod (*Gadus morhua* L.), with particular reference to the development of the stomach and pyloric caeca. J. Fish. Biol. 41 (3), 449–461.
Peng, G.-H., et al., 2005. The photoreceptor-specific nuclear receptor Nr2e3 interacts with Crx and exerts opposing effects on the transcription of rod versus cone genes. Hum. Mol. Genet. 14 (6), 747–764.
Penglase, S., et al., 2015. Diet affects the redox system in developing atlantic COD (*Gadus morhua*) larvae. Redox Biol. 5, 308–318.
Pfaffl, M.W., 2004. Quantification strategies in real-time PCR. AZ Quant. PCR 1, 89–113.
Raymond, P.A., et al., 2014. Patterning the cone mosaic array in zebrafish retina requires specification of ultraviolet-sensitive cones. PLoS One 9 (1), e85325.
Raymond, P.A., Rivlin, P.K., 1987. Germinal cells in the goldfish retina that produce rod photoreceptors. Dev. Biol. 122 (1), 120–138.
Raymond, P.A., Barthel, L.K., Curran, G.A., 1995. Developmental patterning of rod and cone photoreceptors in embryonic zebrafish. J. Comp. Neurol. 359 (4), 537–550.
Rennison, D.J., Owens, G.L., Taylor, J.S., 2012. Opsin gene duplication and divergence in ray-finned fish. Mol. Phylogenet. Evol. 62 (3), 986–1008.
Schmitt, E.A., Dowling, J.E., 1996. Comparison of topographical patterns of ganglion and photoreceptor cell differentiation in the retina of the zebrafish, *Danio rerio*. J. Comp. Neurol. 371 (2), 222–234.
Schmitt, E.A., Dowling, J.E., 1999. Early retinal development in the zebrafish, *Danio rerio*: light and electron microscopic analyses. J. Comp. Neurol. 404 (4), 515–536.
Sotolongo-Lopez, M., et al., 2016. Genetic dissection of dual roles for the transcription factor *six7* in photoreceptor development and patterning in zebrafish. PLoS Genet. 12 (4), p. e1005968.
Star, B., et al., 2011. The genome sequence of Atlantic cod reveals a unique immune system. Nature 477 (7363), 207–210.
Stenkamp, D.L., et al., 1996. Temporal expression of rod and cone opsins in embryonic goldfish retina predicts the spatial organization of the cone mosaic. Investig. Ophthalmol. Vis. Sci. 37 (2), 363–376.
Stenkamp, D.L., et al., 2000. Function for hedgehog genes in zebrafish retinal development. Dev. Biol. 220 (2), 238–252.
Stenkamp, D.L., 2007. Neurogenesis in the fish retina. Int. Rev. Cytol. – Surv. Cell Biol. 259, 173–224.
Stenkamp, D.L., 2011. The rod photoreceptor lineage of teleost fish. Prog. Retin. Eye Res. 30 (6), 395–404.
Stenkamp, D.L., Cameron, D.A., 2002. Cellular pattern formation in the retina: retinal regeneration as a model system. Mol. Vis. 8, 280–293.
Swaroop, A., Kim, D., Forrest, D., 2010. Transcriptional regulation of photoreceptor development and homeostasis in the mammalian retina. Nat. Rev. Neurosci. 11 (8), 563–576.
Szél, Á., et al., 2000. Photoreceptor distribution in the retinas of subprimate mammals. J. Opt. Soc. Am. A 17 (3), 568–579.
Takechi, M., Kawamura, S., 2005. Temporal and spatial changes in the expression pattern of multiple red and green subtype opsin genes during zebrafish development. J. Exp. Biol. 208 (7), 1337–1345.
Takechi, M., Seno, S., Kawamura, S., 2008. Identification of cis-acting elements repressing blue opsin expression in zebrafish UV cones and pineal cells. J. Biol. Chem. 283 (46), 31625–31632.
Temple, S.E., et al., 2008. Effects of exogenous thyroid hormones on visual pigment composition in coho salmon (*Oncorhynchus kisutch*). J. Exp. Biol. 211 (13), 2134–2143.
Tsujimura, T., et al., 2015. Spatially differentiated expression of quadruplicated green-sensitive RH2 opsin genes in zebrafish is determined by proximal regulatory regions and gene order to the locus control region. BMC Genet. 16 (1), 130.
Tsujimura, T., Chinen, A., Kawamura, S., 2007. Identification of a locus control region for quadruplicated green-sensitive opsin genes in zebrafish. Proc. Natl. Acad. Sci. USA 104 (31), 12813–12818.
Tsujimura, T., Hosoya, T., Kawamura, S., 2010. A single enhancer regulating the differential expression of duplicated red-sensitive opsin genes in zebrafish. PLoS Genet. 6 (12), e1001245.
Tupper, M., Boutilier, R., 1995. Effects of habitat on settlement, growth, and post-settlement survival of Atlantic cod (*Gadus morhua*). Can. J. Fish. Aquat. Sci. 52 (9), 1834–1841.
Valen, R., et al., 2014. Molecular evidence that only two opsin subfamilies, the blue light- (SWS2) and green light-sensitive (RH2), drive color vision in Atlantic COD (*Gadus morhua*). PLoS One 9 (12), e115436.
Wan, J., Stenkamp, D.L., 2000. Cone mosaic development in the goldfish retina is independent of rod neurogenesis and differentiation. J. Comp. Neurol. 423 (2), 227–242.
Yokoyama, S., 2000. Molecular evolution of vertebrate visual pigments. Prog. Retin. Eye Res. 19 (4), 385–419.
Young, R.W., 1985. Cell differentiation in the retina of the mouse. Anat. Rec. 212 (2), 199–205.
Zar, J.H., 1996. Biostatistical analisys. Biostatistical Analisys.